Observation of Fermi Pressure in a Gas of Trapped Atoms

Andrew G. Truscott, Kevin E. Strecker, William I. McAlexander,* Guthrie B. Partridge, Randall G. Hulet†

We report the attainment of simultaneous quantum degeneracy in a mixed gas of bosons (lithium-7) and fermions (lithium-6). The Fermi gas has been cooled to a temperature of 0.25 times the Fermi temperature by thermal collisions with the evaporatively cooled bosons. At this temperature, the spatial size of the gas is strongly affected by the Fermi pressure resulting from the Pauli exclusion principle and gives clear experimental evidence for quantum degeneracy.

The experimental achievement of Bose-Einstein condensation (BEC) of trapped atomic gases 5 years ago (*1–3*) catalyzed an explosion of research activity in atoms obeying Bose-Einstein statistics—that is, those with integer spin. In contrast, the pioneering work of DeMarco and Jin (*4*) is so far the only realization of quantum degeneracy in a trapped gas of fermions. Fermions must satisfy the Pauli exclusion principle, which forbids identical particles from occupying the same quantum state. This simple property gives rise to remarkable effects that include the structure of the periodic table of the elements, the nature of electrical conductivity in metals, and the quantum Hall effect. White dwarf and neutron stars manifest the Pauli principle in a striking way. In both cases, the star has exhausted its nuclear fuel and is essentially "dead." Tremendous gravitational forces draw the star in on itself. Inside such a star, however, there is near-unity occupation of the available quantum states (i.e., quantum degeneracy), which provides a "Fermi pressure" that stabilizes the star against collapse (*5*). Here, we report the observation of Fermi pressure in the spatial distribution of a gas of ultracold, trapped atoms.

The lack of experimental realizations of quantum degeneracy in trapped fermions is due to the inability of fermions to be directly evaporatively cooled, a key ingredient in all successful BEC experiments to date. This is because identical fermions are unable to undergo the collisions necessary to rethermalize the gas during evaporation. This obstacle was circumvented in the DeMarco and Jin experiment by simultaneously trapping and evaporatively cooling two different spin states of ^{40}K (*4*). They report that the cooling efficiency decreased, however, when the gas became sufficiently quantum degenerate that rethermalizing collisions were blocked by the diminishing fraction of available unoccupied quantum states, a process known as Pauli blocking (*4*, *6*). In the present work, a mixture of bosons (^{7}Li) and fermions (^{6}Li) is simultaneously cooled to quantum degeneracy. The addition of the bosons enables the fermions to be rethermalized by their elastic interactions with the bosons, and minimizes the Pauli blocking effects.

The present experiment uses standard techniques of laser cooling and trapping, although the complexity is increased because of the addition of a second species. In order to load a magnetic trap, atoms in a thermal beam containing both isotopes are first slowed by laser radiation pressure, by the Zeeman slower technique, and then loaded into a dual magneto-optical trap (MOT). About 3×10^{10} atoms of ^{7}Li are loaded into the MOT in 3 s. Because the laser frequencies needed to trap ^{6}Li interfere with ^{7}Li trapping, the loading of ^{6}Li is limited to no more than 20 ms, during which up to $\sim 10^7$ atoms of ^{6}Li are trapped. Further compression and laser cooling are accomplished by rapidly reducing the intensities and detunings of the trapping laser beams (*7*, *8*). The ^{7}Li atoms are then optically pumped into the $F = 2$, $m_F = 2$ state, which is the desired state for magnetic trapping, whereas the ^{6}Li atoms are optically pumped into the $F = 3/2$ state (*9*). Finally, the laser beams and MOT magnetic fields are switched off while the coils of a cloverleaf-type magnetic trap (*10*) are energized. The magnetic trap is loaded with $\sim 3 \times 10^9$ atoms of ^{7}Li and up to 10^6 atoms of ^{6}Li at 700 μK. The measured axial and radial trapping frequencies for ^{7}Li are $\omega_a = 2\pi \times (39 \pm 1)$ Hz and $\omega_r = 2\pi \times (433 \pm 3)$ Hz, respectively.

Further cooling is accomplished by microwave-induced evaporative cooling of the ^{7}Li (*11*). The ^{6}Li atoms are cooled "sympathetically" through their elastic interactions with the ^{7}Li and are not themselves ejected. The triplet *s*-wave scattering lengths determine the elastic scattering cross sections for thermalization. For ^{7}Li/^{7}Li collisions the scattering length is −1.5 nm, whereas for ^{6}Li/^{7}Li it is 2.2 nm (*12*, *13*). Although neither of these correspond

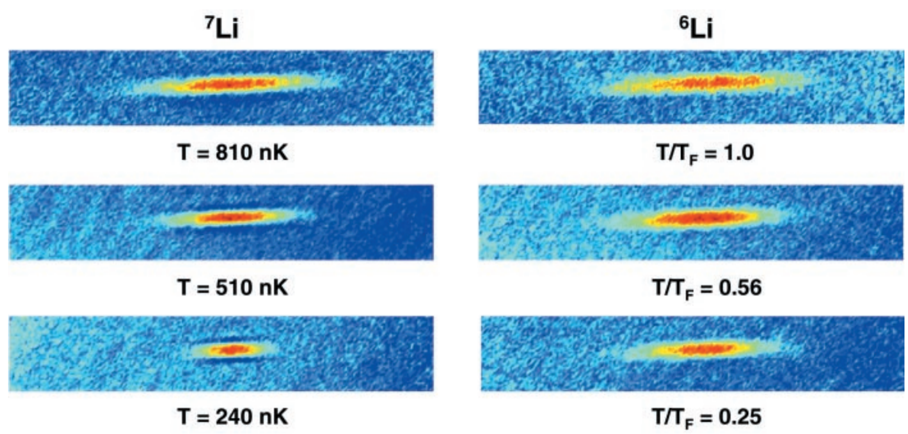

Fig. 1. Two-dimensional false-color images of both ^{7}Li and ^{6}Li clouds. At $T/T_F = 1.0$, the two clouds are approximately the same size, but as the atoms are cooled further, to $T/T_F = 0.56$, the Bose gas contracts, whereas the Fermi gas exhibits only subtle changes in size. At $T/T_F = 0.25$, the size difference between the two gases is clearly discernable. At this temperature the ^{7}Li image displays distortions due to high optical density. However, these distortions are present only in the radial direction and do not affect the measurements. The fitted numbers of ^{7}Li and ^{6}Li atoms, N_7 and N_6, and the fitted temperatures are as follows: For the upper set, $N_7 = 2.4 \times 10^5$, $N_6 = 8.7 \times 10^4$, and $T = 810$ nK; for the middle set, $N_7 = 1.7 \times 10^5$, $N_6 = 1.3 \times 10^5$, and $T = 510$ nK; and for the lower set, $N_7 = 2.2 \times 10^4$, $N_6 = 1.4 \times 10^5$, and $T = 240$ nK. The probe detuning is a parameter of the fits but is constrained to vary by no more than its uncertainty of ±3 MHz. The fits result in typical reduced-χ^2 values of ∼1.0. The uncertainties in number and temperature are due mainly to the uncertainties in the fit and are roughly estimated by finding the point at which the reduced-χ^2 increases by 20%. The resulting uncertainties are 8% in temperature and 15% in number. Other sources of uncertainty are relatively insignificant. The size of each displayed image is 1.00 mm in the horizontal axis and 0.17 mm in the vertical axis.

Department of Physics and Astronomy and the Rice Quantum Institute, Rice University, Houston, TX 77251, USA.

*Present address: Agilent Laboratories, MS 24M-B, Palo Alto, CA 94304–1392, USA.

†To whom correspondence should be addressed. E-mail: randy@atomcool.rice.edu

to particularly large cross sections, they are sufficient to cool both species to quantum degeneracy in ~60 s. Similar methods of sympathetic cooling have been previously used in a two-species ion trap (*14*) and in a two-component Bose gas of ^{87}Rb cooled to BEC (*15*). A recent preprint reports an experiment similar to the present one, in which a ^{6}Li/^{7}Li mixture was sympathetically cooled, although not to quantum degeneracy (*16*).

Once the sympathetic cooling cycle is complete, the atoms are held in the trap for at least 2 s to ensure complete thermalization. The ^{7}Li atoms are then probed with a 7-μs absorption pulse from a laser tuned near the $^2S_{1/2} \leftrightarrow {}^2P_{3/2}$ resonance. The absorption shadow of the ^{7}Li atom cloud is imaged onto a charge-coupled device with a magnification corresponding to 5 μm/pixel. An intense beam, perpendicular to the absorption probe, optically pumps atoms that fall into the lower hyperfine state during imaging to ensure that all atoms contribute to the absorption signal. Immediately after the acquisition of the image, a high-intensity on-resonant optical pulse is applied for 10 μs to quickly remove all remaining ^{7}Li from the magnetic trap. Because the optical pulse is more than 10 GHz detuned from any ^{6}Li resonance, it has no measurable effect on the ^{6}Li atom cloud. The ^{6}Li atoms are then imaged in a similar manner (*17*).

Three pairs of images are shown (Fig. 1) corresponding to three cooling cycles halted at different final temperatures. The number of atoms and their temperature are obtained from the images by fitting them to the appropriate quantum statistical density distribution functions. It is assumed that interactions have a negligible effect on the density. This is a good approximation because ^{7}Li has attractive interactions that limit the number of condensate atoms, and hence the magnitude of the mean field (*11*). This effect also constrains the magnitude of the mean-field experienced by the ^{6}Li as a result of the ^{7}Li, while the self-interaction between the fermions is identically zero in the *s*-wave limit. At the lowest temperatures, the radial dimensions approach the 5-μm resolution of the imaging system, and so only the larger axial dimension is fit. To increase the signal to noise, data within a ±5° angle of the trap axis are averaged. Unlike the fermions, the shape of the density distribution for bosons changes significantly as quantum degeneracy is approached. Even for temperatures somewhat above T_c, the critical temperature for BEC, the boson distribution begins to develop a narrow central component. For this reason, the bosons prove to be a sensitive thermometer for determining the common temperature. The temperature obtained by fitting ^{6}Li to a Fermi-Dirac distribution agrees with that obtained from the ^{7}Li, but with greater uncertainty. Using the boson temperature to constrain the temperature of the Fermi distribution serves to decouple the number and temperature from the fit to the ^{6}Li images, increasing the precision for which the number of ^{6}Li atoms, N_6, can be determined. Temperatures are given relative to the Fermi temperature, which for a harmonic trapping potential is $T_F = \hbar\varpi\,(6N_6)^{1/3}/k_B$ (*18*), where k_B is the Boltzmann constant, $\varpi \equiv (\omega_r^2\omega_a)^{1/3}$, and where the frequencies are adjusted for the ^{6}Li mass.

The doubly spin-polarized ^{6}Li and ^{7}Li atoms have the same magnetic moment, to within a correction on the order of the ratio of the nuclear to the Bohr magneton. At high temperature, therefore, where classical statistics are a good approximation, the spatial distributions should show little difference. Indeed, the upper set of images in Fig. 1, corresponding to T/T_F = 1.0, are nearly indistinguishable. However, in the middle set, with T/T_F = 0.56, the ^{6}Li distribution is slightly broader than that of the ^{7}Li. In the bottom set, corresponding to T/T_F = 0.25, the relative broadening of the ^{6}Li cloud is unmistakable. In all cases, attractive interactions limit the number of ^{7}Li condensate atoms to a small fraction of the total number of ^{7}Li. The ^{7}Li temperature, therefore, cannot go appreciably below T_c. The effect of quantum statistics on the shape and size of the clouds can readily be seen in the axial profiles for

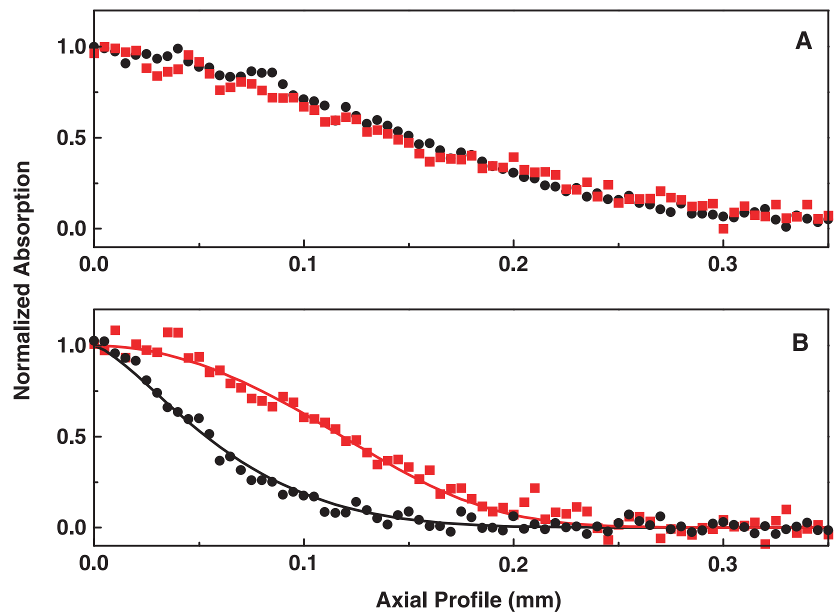

Fig. 2. Comparison of ^{6}Li and ^{7}Li atom cloud axial profiles. The red squares correspond to ^{6}Li, and the black circles to ^{7}Li. (**A**) Data from the top image of Fig. 1, corresponding to T/T_F = 1.0 and T/T_c = 1.5. (**B**) Data from the lower image of Fig. 1, corresponding to T/T_F = 0.25 and T/T_c = 1.0. The fits to the data are shown as solid lines.

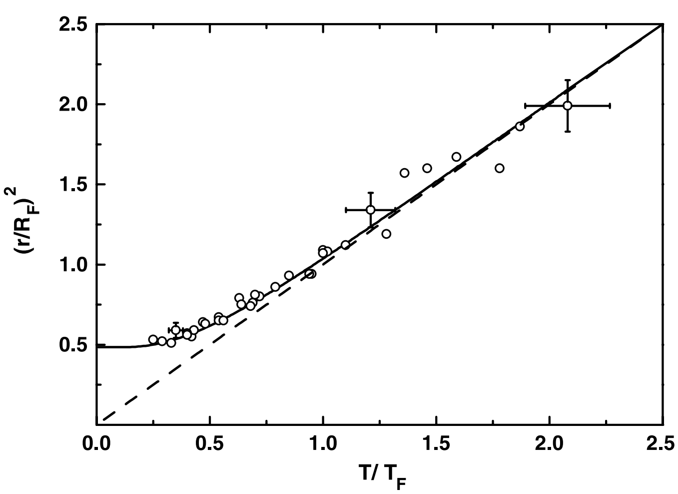

Fig. 3. Square of the 1/*e* axial radius, *r*, of the ^{6}Li clouds versus T/T_F. The radius is normalized by the Fermi radius, $R_F = (2k_BT_F/m\omega_a^2)^{1/2}$, where *m* is the atomic mass of ^{6}Li. The solid line is the prediction for an ideal Fermi gas, whereas the dashed line is calculated assuming classical statistics. The data are shown as open circles. The divergence of the data from the classical prediction is the result of Fermi pressure. Several representative error bars are shown. These result from the uncertainties in number and temperature as described in the legend to Fig. 1. In addition, we estimate an uncertainty of 3% in the determination of *r*.

$T/T_F = 1.0$ and 0.25 (Fig. 2, A and B, respectively). The deviations in the size and shapes of these clouds highlight their dissimilar quantum statistical nature.

The square of the radius of the ^{6}Li clouds is plotted versus T/T_F (Fig. 3), where it can be seen that at relatively high temperatures, the radius decreases as $T^{1/2}$, as expected for a classical gas (dashed line). At a temperature near 0.5 T_F, however, the radius is seen to deviate from the classical prediction, and at the lowest temperatures, to plateau to ~0.7 times the Fermi radius. At $T = 0$, every trap state is singly occupied up to the Fermi energy, giving rise to a nonzero mean energy and a resulting Fermi pressure. Fermi pressure is responsible for the minimum radius and is a dramatic manifestation of Fermi-Dirac statistics.

Thermal equilibrium between the ^{6}Li and ^{7}Li clouds is assumed in the analysis presented here. To investigate this assumption, the delay between the end of evaporation and the recording of an image was delayed by up to 10 s. No deviations from thermal equilibrium were observed either for the longest delays or for images recorded immediately after evaporation, indicating that the ^{6}Li and ^{7}Li are in thermal equilibrium throughout the evaporation process. At the lowest temperatures and densities, the calculated time for elastic collisions between a ^{6}Li atom and ^{7}Li is ~0.5 s. To ensure complete equilibration, all data presented here for $T/T_F < 1$ used a 5-s delay, whereas a 2-s delay was used for the hotter data.

Sympathetic cooling of a Fermi gas by a Bose gas has several advantages compared with direct evaporative cooling of a two-component Fermi gas (*4*, *6*, *19*). As previously mentioned, bosons provide superior temperature sensitivity and help to minimize the rethermalization-inhibiting Pauli blocking effects. Furthermore, the loss of fermions during the cooling cycle is minimized because they are not actively removed. Sympathetic cooling of the Fermi gas becomes inefficient, however, when the heat capacity of the Bose gas, which diminishes as atoms are evaporated, drops below that of the Fermi gas. The limit of sympathetic cooling in our experiment may be estimated by finding the conditions at which both heat capacities are equal. Because attractive interactions limit the number of condensate atoms to less than 1000 for the present experiment, the condensate fraction is small and, to a good approximation, the minimum achievable temperature is T_c (*11*). The heat capacity for a harmonically confined gas of N_B bosons at T_c is $C_B = 10.86\ N_B k_B$ (*20*), whereas for a Fermi gas below ~0.5 T_F the heat capacity is $C_F = \pi^2 N_F k_B (T/T_F)$ (*18*). Equating the heat capacities implies that cooling N_F fermions becomes inefficient when the number of bosons is decreased below $N_F(T/T_F)$. This assertion is supported by our most degenerate data, $T/T_F = 0.25$, for which $N_B = 2.2 \times 10^4$ and $N_F = 1.4 \times 10^5$, where intentionally less than the maximum number of ^{6}Li atoms were loaded. Because N_B is related to T_c, and N_F to T_F, it can be shown that the condition $C_B > C_F$ implies that $T/T_F \geq 0.3$, which is again consistent with observations, assuming that evaporation can extend somewhat beyond the point of equality of the heat capacities. This limitation may be overcome by simultaneously evaporating the fermions. The lack of good spatial overlap between the Fermi gas and the Bose-Einstein condensate and superfluidity of the condensate may become important as the temperature is reduced further (*21, 22*).

The attainment of a quantum-degenerate Fermi gas presents several exciting opportunities. For instance, a mixed Bose/Fermi gas may phase-separate at very low temperatures (*23*, *24*), similar to phase separation in mixtures of liquid ^{4}He/^{3}He (*25*). Also in analogy with liquid helium mixtures (*25*), a fermionic impurity atom may be useful as a probe of bosonic superfluidity (*21*). One of the most intriguing opportunities, however, is the possibility of observing a Bardeen-Cooper-Schrieffer (BCS) phase transition to a superfluid state (*26–28*). Such a transition would be analogous to superconductivity in solids and to superfluidity in liquid ^{3}He. In contrast to solids and liquids, however, interactions in trapped atomic gases are weak and tunable, making them nearly ideal environments for comparison with theory. ^{6}Li is especially well suited for such an experiment, in which a two-component spin mixture would undergo *s*-wave Cooper pairing at sufficiently low temperature (*26*, *28*), because its triplet *s*-wave interaction is both attractive and enormous (*12*, *19*). Furthermore, magnetically tuned Feshbach resonances (*29*) have been identified theoretically for ^{6}Li at modest magnetic field strengths (*13*, *30*), and these could provide an experimentally tunable "knob" for controlling the interaction strength and sign. Use of such a Feshbach resonance may allow tuning of the BCS transition temperature into the regime reported here.

References and Notes

1. M. H. Anderson, J. R. Ensher, M. R. Matthews, C. E. Wieman, E. A. Cornell, *Science* **269**, 198 (1995).
2. C. C. Bradley, C. A. Sackett, J. J. Tollett, R. G. Hulet, *Phys. Rev. Lett.* **75**, 1687 (1995).
3. K. B. Davis *et al.*, *Phys. Rev. Lett.* **75**, 3969 (1995).
4. B. DeMarco, D. S. Jin, *Science* **285**, 1703 (1999).
5. S. L. Shapiro, S. A. Teukolsky, *Black Holes*, *White Dwarfs*, *and Neutron Stars*, *The Physics of Compact Objects* (Wiley, New York, 1983).
6. M. J. Holland, B. DeMarco, D. S. Jin, *Phys. Rev. A* **61**, 053610 (2000).
7. M.-O. Mewes, G. Ferrari, F. Schreck, A. Sinatra, C. Salomon, *Phys. Rev. A* **61**, 011403(R) (1999).
8. The ^{7}Li MOT is formed by six laser beams, each with two frequencies. One frequency is detuned 42 MHz red of the $S_{1/2}$, F = 1 ↔ $P_{3/2}$, F′ = 2 transition, with a central intensity of 4 mW/cm^2 per beam. The other is detuned 42 MHz red of the $S_{1/2}$, F = 2 ↔ $P_{3/2}$, F′ = 3 transition, with a central intensity of 1.3 mW/cm^2 per beam. The ^{6}Li MOT uses laser frequencies detuned 12 MHz red of the $S_{1/2}$, F = 1/2 ↔ $P_{3/2}$, F′ = 3/2 transition, and 30 MHz red of the $S_{1/2}$, F = 3/2 ↔ $P_{3/2}$, F′ = 5/2 transition, with intensities of 0.7 mW/cm^2 and 2 mW/cm^2 per beam, respectively. The compression and cooling stage has the following sequence: The ^{6}Li F = 1/2 light intensity is reduced by a factor of 10, and the ^{7}Li F = 1 light intensity is reduced by a factor of 100. The detuning of the ^{7}Li F = 2 light is then ramped from 42 to 12 MHz in 3 ms. Finally, the intensities of the ^{7}Li MOT beams are reduced by a factor of 10 and left on for 3 ms.
9. The optical pumping happens in two stages. The ^{6}Li is first pumped into the $S_{1/2}$, F = 3/2 state by pulsing on the MOT beams resonant with the F = 1/2 ground state for 100 μs. Then, the ^{7}Li is pumped into the F = 2 ground state with a 200-μs pulse resonant with the F = 1 ground state. Second, a circularly polarized pulse containing both the ^{7}Li F = 1 and F = 2 frequencies is applied along the magnetic quantization axis for 500 μs, pumping the ^{7}Li atoms into the desired F = 2, m_F = 2 magnetic sublevel. Although the ^{6}Li is prepared in a mixture of F = 3/2 sublevels, all but the desired F = 3/2, m_F = 3/2 population quickly decay through spin-exchange collisions with the ^{7}Li.
10. M.-O. Mewes *et al.*, *Phys. Rev. Lett.* **77**, 416 (1996).
11. C. A. Sackett, C. C. Bradley, M. Welling, R. G. Hulet, *Appl. Phys. B* **65**, 433 (1997).
12. E. R. I. Abraham *et al.*, *Phys. Rev. A* **55**, R3299 (1997).
13. F. A. van Abeelen, B. J. Verhaar, A. J. Moerdijk, *Phys. Rev. A.* **55**, 4377 (1997).
14. D. J. Larson, J. C. Bergquist, J. J. Bollinger, W. M. Itano, D. J. Wineland, *Phys. Rev. Lett.* **57**, 70 (1986).
15. C. J. Myatt, E. A. Burt, R. W. Ghrist, E. A. Cornell, C. E. Wieman, *Phys. Rev. Lett.* **78**, 586 (1997).
16. F. Schreck *et al.*, available at http://arXiv.org/abs/cond-mat/0011291.
17. The ^{7}Li probe has a detuning of 12 ± 3 MHz with an intensity of 2.5 ± 0.3 mW/cm^2. The ^{6}Li probe has a detuning of 11 ± 3 MHz with the same intensity.
18. D. A. Butts, D. S. Rokhsar, *Phys. Rev. A* **55**, 4346 (1997).
19. K. M. O'Hara, M. E. Gehm, S. R. Granade, S. Bali, J. E. Thomas, *Phys. Rev. Lett.* **85**, 2092 (2000).
20. V. Bagnato, D. E. Pritchard, D. Kleppner, *Phys. Rev. A* **35**, 4354 (1987).
21. E. Timmermans, R. Côté, *Phys. Rev. Lett.* **80**, 3419 (1998).
22. W. Geist, L. You, T. A. B. Kennedy, *Phys. Rev. A* **59**, 1500 (1999).
23. K. Mølmer, *Phys. Rev. Lett.* **80**, 1804 (1998).
24. M. Amoruso, A. Minguzzi, S. Stringari, M. P. Tosi, L. Vichi, *Eur. Phys. J. D* **4**, 261 (1998).
25. K. H. Bennemann, J. B. Ketterson, *The Physics of Liquid and Solid Helium* (Wiley, New York, 1976).
26. H. T. C. Stoof, M. Houbiers, C. A. Sackett, R. G. Hulet, *Phys. Rev. Lett.* **76**, 10 (1996).
27. M. A. Baranov, Y. Kagan, M. Y. Kagan, *JETP Lett.* **64**, 301 (1996).
28. A. G. W. Modawi, A. J. Leggett, *J. Low Temp. Phys.* **109**, 625 (1998).
29. E. Tiesinga, B. J. Verhaar, H. T. C. Stoof, *Phys. Rev. A* **47**, 4114 (1993).
30. M. Houbiers, H. T. C. Stoof, W. I. McAlexander, R. G. Hulet, *Phys. Rev. A* **57**, R1497 (1998).

31. Supported by the Office of Naval Research, NASA, the National Science Foundation, and the R. A. Welch Foundation. We are grateful to B. Ghaffari and D. Homan for their help in constructing the apparatus.

25 January 2001; accepted 16 February 2001
Published online 1 March 2001;
10.1126/science.1059318
Include this information when citing this paper.